Acknowledgment. This work was supported by NSF Grant CHE 9119910.

Supplementary Material Available: For the X-ray studies of **1** and **2**, tables of crystal data and experimental conditions, atomic positional parameters, bond lengths, bond angles, and anisotropic temperature factors (11 pages); tables of calculated and observed structure factors (8 pages). Ordering information is given on any current masthead page.

Department of Chemistry
Syracuse University
Syracuse, New York 13244

M. Ishaque Khan
Qin Chen
Jon Zubieta*

Exxon Research and Engineering Company
Annandale, New Jersey 08801

David P. Goshorn

Received January 29, 1992

Articles

Contribution from the Dipartimento di Chimica Inorganica, Metallorganica ed Analitica, Università di Padova, Padova, Italy, Dipartimento di Scienze Chimiche, Università di Catania, Catania, Italy, and Istituto di Chimica e Tecnologia dei Radioelementi, CNR, Padova, Italy

$Zn_4O(acetate)_6$, a Well-Tailored Molecular Model of ZnO. An Experimental and Theoretical Investigation of the Electronic Structure of $Zn_4O(acetate)_6$ and ZnO by Means of UV and X-ray Photoelectron Spectroscopies and First Principle Local Density Molecular Cluster Calculations

Renzo Bertoncello,[1a] Marco Bettinelli,[1a] Maurizio Casarin,*[,1a] Antonino Gulino,[1b] Eugenio Tondello,[1a] and Andrea Vittadini[1c]

Received November 21, 1991

A thorough investigation of the electronic structure of $Zn_4O(acetate)_6$ and ZnO has been used to test the hypothesis that the former compound is a well-tailored molecular model of the latter solid. First principle local density molecular cluster calculations relative to $Zn_4O(acetate)_6$ and ZnO indicate that the tetrahedral arrangement of four Zn atoms around the central oxygen present in the title compound is a very good model of the oxygen chemical environment in ZnO. Furthermore, the obtained theoretical results allowed us to describe the rather complex nature of the lowest energy electronic absorption transition of $Zn_4O(acetate)_6$, pointing out once more the leading role played by the tetrahedral arrangement of the central oxygen to explain the observed optical properties. Moreover, the computed different electronic charges found in the nearest volume surrounding unlike oxygen atoms in $Zn_4O(acetate)_6$ and transition state ionization energies were found to agree very well with X-ray and UV photoelectron measurements, respectively. Quite surprisingly, a satisfactory description of the electronic structure of the solid ZnO by means of the $OZn_4O_{12}^{18-}$ cluster, embedded in the ZnO crystalline potential, was obtained only by using an extended basis set for the oxygen atoms, including their 3s and 3p virtual levels. In such a case, the agreement between the computed Zn and O partial density of states, the HOMO-LUMO ΔE, and literature experimental data was excellent and allowed to gain new insights into the Zn-O covalent interaction.

Introduction

In the last decade several theoretical molecular cluster investigations have been devoted to the study of the electronic structure of metal oxides and of defect centers in these materials.[2] Actually, a common feature of these oxides is their nonstoichiometry as a consequence of a significant percentage of oxygen vacancies which combine to determine the electronic properties of these materials.[3] In such cases, the molecular cluster approach is not only computationally attractive with respect to the ordinary band structure approximation but also physically reasonable, obviously by providing suitable boundary conditions, because it allows one to obtain a detailed estimate of the local values of the potential very close to the crystal structure defect.

In a recent contribution Kunkely and Vogler[4] reported the electronic absorption and emission spectra in the visible and UV regions of an EtOH solution of $Zn_4O(acetate)_6$ [(μ_4-oxo)hexakis(μ-acetato)tetrazinc], which was assumed to be a well-suited molecular model of ZnO. An interesting feature of the experimental data they measured was the relative highly efficient luminescence (quantum yield $\phi = 0.15$ in solution at room temperature) for a compound containing the formally closed shell d^{10} Zn^{2+} ion. Moreover, it is worth of note that Blasse et al.[5,6] reported and discussed in the near past the emission and excitation spectra in the visible and UV regions of crystalline $Zn_4O(BO_2)_6$, which also shows a relatively high luminescence efficiency at room temperature.

Both $Zn_4O(acetate)_6$ and $Zn_4O(BO_2)_6$ are characterized by the presence of an oxygen ion at the center of a tetrahedron of zinc ions tetrahedrally coordinated by oxygen (see Figure 1a),[7,8] so

(1) (a) Università di Padova. (b) Università di Catania. (c) CNR.
(2) (a) Walch, P. F.; Ellis, D. E. *Phys. Rev. B* **1973**, *8*, 5920. (b) Kutzler, F. W.; Ellis, D. E. *Phys. Rev. B* **1984**, *29*, 6890. (c) Chou, S.-H.; Guo, J.; Ellis, D. E. *Phys. Rev. B* **1986**, *34*, 12. (d) Press, M. R.; Ellis, D. E. *Phys. Rev. B* **1987**, *35*, 4438. (e) Khowash, P. K.; Ellis, D. E. *Phys. Rev. B* **1987**, *36*, 3394. (f) Shangda, X.; Changxin, G.; Libin, L.; Ellis, D. E. *Phys. Rev. B* **1987**, *35*, 7671. (g) Khowash, P. K.; Ellis, D. E. *Phys. Rev. B* **1989**, *39*, 1908. (h) Ellis, D. E.; Lam, D. J. *Physica B* **1988**, *150*, 25. (i) Goodman, G. L.; Ellis, D. E.; Alp, E. E.; Soderholm, L. *J. Chem. Phys.* **1989**, *91*, 2983. (j) Guo, J.; Ellis, D. E.; Goodman, G. L.; Alp, E. E.; Soderholm, L.; Shenoy, G. K. *Phys. Rev. B* **1990**, *41*, 82.
(3) (a) Banus, M. D.; Reed, T. B.; Strauss, A. J. *Phys. Rev. B* **1972**, *5*, 2775. (b) Hayakawa, M.; Cohen, J. B.; Reed, T. B. *J. Am. Ceram. Soc.* **1972**, *55*, 160. (c) Dieckmann, R. *Z. Phys. Chem. (Neue Folge)* **1977**, *107*, 189. (d) Fisher, B.; Tannhauser, D. S. *J. Chem. Phys.* **1965**, *44*, 1663. (e) von Schwier, G.; Dieckmann, R.; Schnmalzried, H. *Ber. Bunsen-Ges. Phys. Chem.* **1973**, *77*, 402. (f) von Schwier, G.; Schnmalzried, H. *Ber. Bunsen-Ges. Phys. Chem.* **1973**, *77*, 721.
(4) Kunkely, H.; Vogler, A. *J. Chem. Soc., Chem. Commun.* **1990**, 1204.
(5) Meijerink, A.; Blasse, G.; Glasbeek, M. *J. Phys.: Condens. Matter* **1990**, *2*, 6303.
(6) Blasse, G. *Chem. Phys. Lett.* **1990**, *175*, 237.
(7) Hiltunen, L.; Leskelä, M.; Mäkelä, M.; Niinistö, L. *Acta Chem. Scand., A* **1987**, *41*, 548.
(8) Bohaty, L.; Haussül, S.; Liebertz, J.; Stähr, S. *Z. Kristallogr.* **1980**, *151*, 175.

0020-1669/92/1331-1558$03.00/0

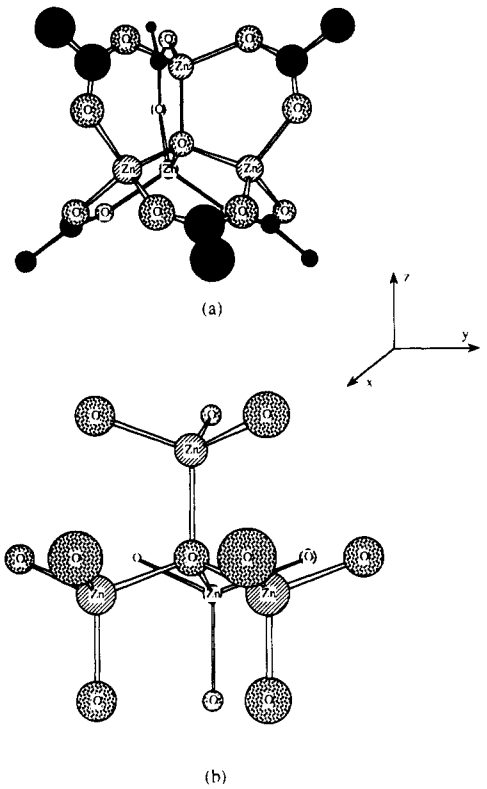

Figure 1. (a) Schematic representation of $Zn_4O(acetate)_6$; (b) Schematic representation of the 17-atom cluster OZn_4O_{12} used to simulate the hexagonal ZnO.

that the high similarity of their spectral properties can be confidently attributed to the presence of that particular cluster of atoms. Furthermore, the chemical environment of the central oxygen anion and of the four zinc cations makes, on a structural basis, $Zn_4O(acetate)_6$ a well-tailored molecular model of zincite (hexagonal ZnO).

In this contribution we report the results of an experimental and theoretical investigation of the electronic structure of $Zn_4O(acetate)_6$ carried out by coupling UV gas-phase and X-ray solid-state photoelectron spectroscopy to high-quality self-consistent local density molecular cluster calculations.[9] Moreover, a series of numerical experiments, carried out by using the same theoretical approach employed for the molecular compound, within the cluster embedded procedure,[10] have been also performed on the cluster $OZn_4O_{12}^{18-}$, as representative of the hexagonal ZnO, to investigate the electronic properties of the solid. The comparison of experimental and theoretical data relative to $Zn_4O(acetate)_6$ with those pertinent to the crystalline ZnO is particularly interesting for the following reasons: (i) it allows us to verify the hypothesis, simply based on crystal structure arguments, that $Zn_4O(acetate)_6$ is a molecular model of ZnO; (ii) it allows us to gain new insights into the optical properties of ZnO by investigating the spectroscopy and the electronic structure of $Zn_4O(acetate)_6$; (iii) finally, it allows us to verify how reliable is the cluster embedding procedure for investigation of the electronic structure of II–VI materials.

Experimental Section

Calculations Details. The quantum mechanical calculations have been run within the self-consistent one-electron local density approach. The nonrelativistic form of the one-electron Schrödinger equation can be written (in Hartree atomic units; σ represents spin) as

$$H_\sigma \Psi_{i\sigma}(\mathbf{r}) = \epsilon_{i\sigma} \Psi_{i\sigma}(\mathbf{r}) \qquad (1)$$

where

$$H_\sigma = [-\tfrac{1}{2}\nabla^2 + V_c(\mathbf{r}) + V_{xc,\sigma}(\mathbf{r})] \qquad (2)$$

The three terms refer to the kinetic energy, the Coulomb potential, and the exchange-correlation potential, respectively. As far as the effective single particle exchange-correlation potential is concerned, the von Barth–Hedin approximation[11] has been used throughout the paper.

The matrix elements of the effective Hamiltonian and of the symmetry orbital overlap matrix S are evaluated as discrete sums over a set of sample points. This set includes not only pseudorandom diophantine points[12,13] but also a regular spherical volume mesh which has been added in order to obtain a better accuracy in the description of the wave function in the region close to the nuclei.

Two different procedures were employed to approximate the cluster electron charge density for the $Zn_4O(acetate)_6$ and the crystalline ZnO. In particular, in the latter case, the discrete variational (DV) approach has been employed to determine the wave functions and the eigenvalues of an embedded cluster. In this scheme the rest of the solid is mimicked by providing an electrostatic crystal field and charge field in which the cluster is embedded. This is done by generating a microcrystal surrounding the cluster and placing the atoms at specified lattice positions. Self-consistency is then used to create a Coulomb and exchange-correlation potential in which the cluster is immersed. A theoretical description of the cluster embedded procedure can be found in ref 10. For the purposes of the present contribution it is sufficient to mention that the crucial point of such a procedure is that of limiting surface or cluster size effects by making the peripheral atoms sense a potential similar to that found in the bulk crystal. Moreover, keeping in mind that we are interested in verifying the capability of the OZn_4O_{12} fragment of $Zn_4O(acetate)_6$ to simulate the electronic properties of ZnO, the representation of the extended solid by a "small", embedded cluster is, as already pointed out, not only computationally attractive but also physically reasonable.

The occupation numbers of each molecular orbital (MO) have been determined by applying Fermi–Dirac statistics. The Coulomb potential has been computed by a one-dimensional integration by replacing the actual electron charge density with a model density. Once more two different approximations have been used for the isolated molecule and the extended system. In the former, the "true" electron charge density has been cast in a multicenter overlapping multipolar form,[14] while in the latter an approximate spherical-superposition charge density, resulting from a linear combination of atomic radial densities, has been used to model the actual charge density in ZnO. The expansion (or "population") coefficients have been determined by a least-square fit to the cluster charge density obtained from the occupied wave functions that are solutions of the system Hamiltonian.

The self-consistent potential and the charge density of the cluster $OZn_4O_{12}^{18-}$ have been averaged over the different Zn and O atoms separately in order to take care of the presence of a single type of Zn and O centers in the crystalline ZnO. The evaluation of the total nonspherical Coulomb potential has been carried out by summing over all the spherically symmetric contributions of all the atoms of the microcrystal, obtained by using a generalized Ewald-type summation.[15] More details about the applications of this procedure to the investigation of the electronic properties of metal oxides can be found in ref 2d.

Numerical atomic orbitals (AOs) generated by Hartree–Fock–Slater calculations on free neutral/ionic atoms were used as basis functions. Both in $Zn_4O(acetate)_6$ and in ZnO SCF calculations an extended basis set has been used for Zn and O atoms (1s–4d and 1s–3p, respectively), while a minimal basis set for C and H has been adopted in the former case. Spherical wells (2 Ry deep) having an internal and external radius of 4.0 and 6.0 au, respectively, were added to the atomic potentials. Such a procedure provides a practical means for extending the basis to deal with diffuse orbitals. Moreover, it is flexible enough so that the basis sets can be optimized for the particular molecular application.

To evaluate the magnitude of the electronic relaxation associated with the excitation or the ionization of one electron from the various ground-state MOs, transition-state (TS) calculations using the Slater TS formalism[16] have been carried out.

The experimental geometry of the molecular compound[7] has been idealized to C_{3v} symmetry even though it is worthwhile to mention that

(9) (a) Casarin, M.; Granozzi, G.; Tondello, E.; Vittadini, A. *Chem. Phys.* **1991**, *154*, 385; (b) Ajð, D.; Casarin, M.; Granozzi, G.; Tondello, E.; Vittadini, A. *Int. J. Mater. Prod. Technol.*, in press.
(10) Ellis, D. E.; Benesh, G. A.; Byrom, E. *Phys. Rev. B* **1977**, *16*, 3308.
(11) von Barth, U.; Hedin, L. *J. Phys. C* **1972**, *5*, 1629.
(12) (a) Ellis, D. E. *Int. J. Quantum Chem.* **1968**, *S2*, 35. (b) Ellis, D. E.; Painter, G. S. *Phys. Rev. B* **1970**, *2*, 2887.
(13) Haselgrove, C. B. *Math. Comput.* **1961**, *15*, 323.
(14) Delley, B.; Ellis, D. E. *J. Chem. Phys.* **1982**, *76*, 1949.
(15) Tosi, M. P. in *Solid State Physics*; Seitz, F., Turnbull, D., Ed.; Academic: New York, 1964; Vol. 16, p 1.
(16) Slater, J. C. *Quantum Theory of Molecules and Solids. The Self-Consistent Field For Molecules and Solids*; McGraw-Hill: New York, 1974; Vol. 4.

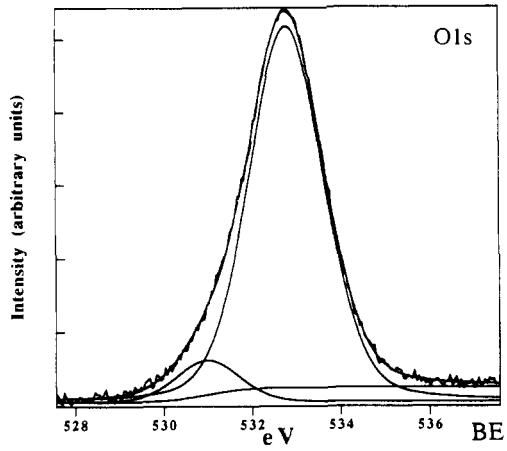

Figure 2. XPS O_{1s} spectrum (MgKα) of $Zn_4O(acetate)_6$.

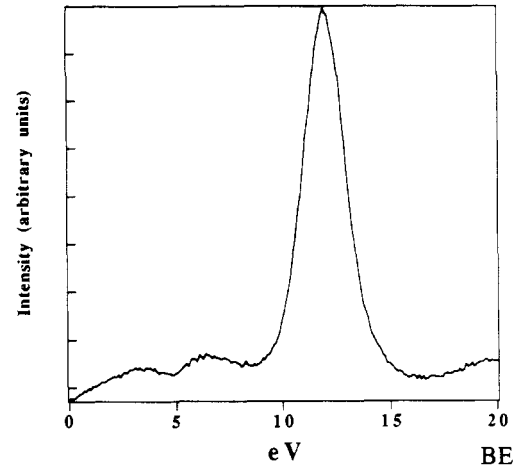

Figure 3. XPS valence band (MgKα) of $Zn_4O(acetate)_6$ with respect to the corrected Fermi level.

the lowering of the molecular symmetry from T_d to C_{3v} is only due to the methyl hydrogens. For this reason the self-consistent potential and the charge density have been averaged over the different zinc atoms, the different oxygens and carbons of the carboxylate groups and the different carbons of the methyls in order to minimize size effects.

A 17-atom cluster of C_{3v} symmetry (the z axis is coincident with a O–Zn bond, see Figure 1b) consisting of a central oxygen (O_1) and two shells of nearest neighbors (four Zn and twelve O atoms, respectively) has been used to mimic the crystalline ZnO. Geometrical parameters relative to the employed cluster have been taken from ref 17, where the crystal structure of hexagonal ZnO is reported. At this regard, we have to point out that the ideal c/a ratio (1.633) rather than the experimental one (1.602) for the ZnO hexagonal close-packed crystalline lattice has been assumed. Such a ratio gives rise to a Zn–O internuclear distance of 1.978 Å to be compared with the experimental ones of 1.992 and 1.973 Å.[17] It is worthy of note that the experimental mean value of the Zn–O internuclear distance corresponds to the one we used. The microcrystal, i.e. the set of crystal atoms around the cluster providing the self-consistent crystal field in which the cluster is embedded, consists of 266 of the nearest oxygen (133) and zinc atoms.

Finally, instead of displaying discrete eigenvalues along an energy axis, we have plotted the density of states (hereafter DOS) as a function of energy. Expressions 3 and 4 refer to the partial and total density of states

$$\mathrm{PDOS}^{v}_{nl}(\epsilon) = \sum_{p} f^{v}_{nl,p} \frac{\gamma/\pi}{(\epsilon - \epsilon_p)^2 + \gamma^2} \tag{3}$$

$$\mathrm{DOS}(\epsilon) = \sum_{v,n,l} \mathrm{PDOS}^{v}_{nl}(\epsilon) = \sum_{p} \frac{g_p \gamma/\pi}{(\epsilon - \epsilon_p)^2 + \gamma^2} \tag{4}$$

(PDOS, DOS), respectively, where $f^{v}_{nl,p}$ is the Mulliken population[18] contribution from atom v, state (nl) to the pth MO of energy ϵ_p and degeneracy g_p. The Lorentzian broadening factor γ, set to 0.3 eV, allows the smoothing of the discrete level structure to simulate solid-state bands. These plots have the advantage of providing insights into the disposition and composition of energy levels over a broad range of energy.

The calculations have been performed on a work station DEC5200/CX (DIGITAL Equipment) at the Inorganic Chemistry Department of the University of Padova.

Synthesis. The sample used for the UV photoelectron spectroscopy (UV–PES) investigation, kindly supplied by Prof. A. Vogler, was synthesized according to the published procedure[19] and recrystallized from C_6H_6 prior to use.

Spectra. The XPS O_{1s} spectrum and the XPS valence band region of $Zn_4O(acetate)_6$ are shown in Figures 2 and 3, respectively. The experimental analyses were performed in a VG Escalab MK II system equipped with nonmonochromatized Mg Kα (1253.6 eV) and Al Kα (1486.6 eV) X-ray sources, in the 10^{-8} Pa residual pressure range. The measurements were carried out on a sample obtained by thermal decomposition of $Zn(acetate)_2{\cdot}2H_2O$ at 180 °C in inert atmosphere (N_2) at 10^{-1} Pa followed by sublimation on a gold thin plate.[7] The electron spectrometer was calibrated by assuming the binding energy (BE) of the gold $4f_{7/2}$ line at 84.0 eV with respect to the Fermi level.[20] Owing to surface charging, the sample presents an average shift of the signal energies of about 5 eV. These charging effects have been corrected for by the internal reference method, i.e., the carbon 1s line (BE = 284.8 eV)[21] of the "adventitious" hydrocarbon layer adsorbed on the sample surface.

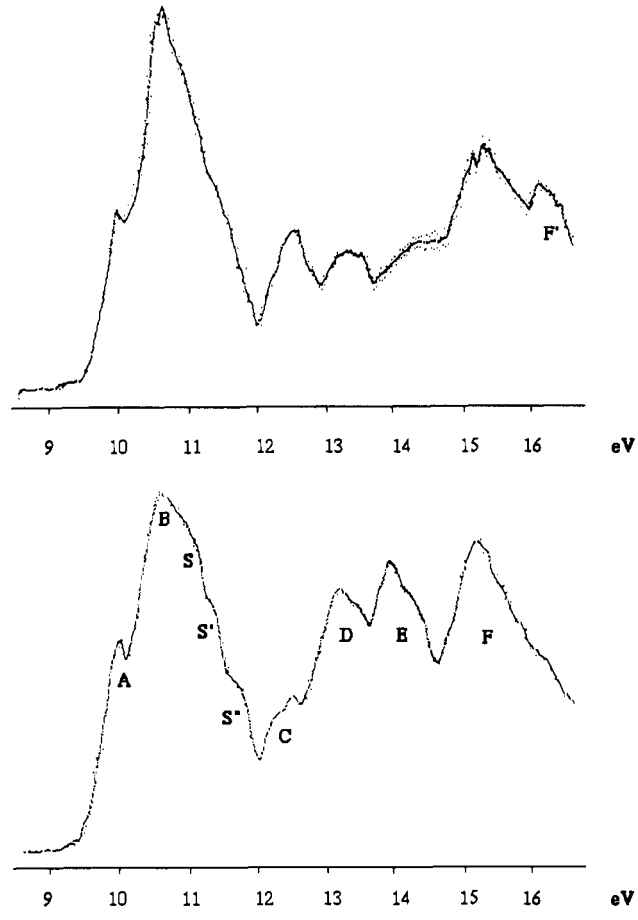

Figure 4. He I (bottom)/He II (top) PE spectra of $Zn_4O(acetate)_6$.

He I and He II gas-phase PE spectra of $Zn_4O(acetate)_6$ are reported in Figure 4 where bands have been alphabetically labeled. The PE spectra were recorded by directly interfacing an IBM AT computer to a Perkin-Elmer PS-18 spectrometer modified for He II measurements by inclusion of a hollow cathode discharge lamp giving high output of He II photons (Helectros Developments). Resolution measured on the He $1s^{-1}$ line was always around 22 meV. The He II spectra were corrected only for the He IIβ "satellite" contributions (10% on reference N_2

(17) Abrahams, S. C.; Bernstein, J. L. *Acta Crystallogr., B* **1969**, *25*, 1233.
(18) Mulliken, R. S. *J. Chem. Phys.* **1955**, *23*, 1833.
(19) Putt, H.; Sievers, R. In *Handbuch der Präparativen Anorganischen Chemie*; Brauer, G., Ed.; Ferdinand Enke Verlag: Stuttgart, 1978.
(20) Anthony, M. T.; Seah, M. P. *Surf. Interface Anal.* **1984**, *6*, 95.
(21) Seah, M. P. In *Practical Surfaces Analysis*, 2nd ed.; Briggs, D., Seah, M. P., Eds.; Wiley: Chichester, U.K., 1990; Vol. 1.

Table I. SCM DV Atomic Character for $Zn_4O(acetate)_6$[a]

eigenvalue			population, %							
			O′		4Zn			12O″		
MO	$-\epsilon$, eV	-TSIE, eV	s	p	s	p	d	s	p	$6CCH_3$
$11a_2$	2.62		0	0	0	1	1	0	64	34
34e	2.68		0	0	0	1	1	0	55	33
33e	3.03		0	−3	0	5	5	1	59	33
$24a_1$	3.03		33	0	27	3	1	13	16	7
$23a_1$*	3.07		0	0	0	3	3	1	50	43
$22a_1$	8.15	10.28	0	10	0	0	9	0	76	5
32e	8.17	10.30	0	6	0	0	6	0	81	7
31e	8.43	10.56	0	10	0	0	8	0	75	7
$10a_2$	8.52	10.65	0	0	0	0	3	0	93	4
$21a_1$	8.59	10.72	0	14	0	1	9	1	57	18
30e	8.72	10.85	0	2	0	1	7	0	75	15
29e	8.84	10.97	0	5	0	1	8	0	69	17
$9a_2$	9.01	11.14	0	0	0	0	0	0	100	0
28e	9.23	11.36	0	0	0	0	2	0	92	6
$8a_2$	9.30	11.43	0	0	0	0	2	0	98	0
27e	9.59	11.72	0	0	0	2	1	1	87	9
$20a_1$	9.75	11.88	1	0	8	0	8	3	52	28
$19a_1$	10.62	12.75	2	33	4	6	18	2	21	14
26e	10.68	12.82	0	26	8	11	21	4	17	13
25e	11.24	13.37	0	0	0	2	38	6	23	31

[a] Lowest unoccupied MO.

spectrum). The ionization energy (IE) scale was calibrated by reference to peaks due to admitted inert gases (Xe–Ar) and to the He $1s^{-1}$ self-ionization. A heated inlet probe system was adopted at 180 °C.

Results and Discussion

$Zn_4O(acetate)_6$. In Table I the ground-state charge density analysis of the outermost MOs of $Zn_4O(acetate)_6$ is reported together with the TS ionization energies (hereafter TSIEs). A TS calculation was performed only for the $^2A_1$ state (ionization from the $22a_1$ highest occupied MO (HOMO)), while the remaining TSIEs were evaluated under the assumption that similar relaxations as in this $^2A_1$ state occur. Among the occupied levels, the last 23 ones (considering their degeneracies) have been included in Table I in order to be sure of picking up all the linear combinations coming from the π_2 ($2a_2 + 2e$), n^+ ($a_1 + 2e$) and n^- ($a_1 + a_2 + 2e$) levels mainly localized on the oxygen atoms of the carboxylic groups (O″). According to that, the orbitals ranging from the $22a_1$ MO to the $20a_1$ one are strongly localized on O″. Unfortunately, it was impossible to assign a particular character (π_2, n^+, n^-) to the reported MOs because of the extensive mixing between levels of the same symmetry.

Among the reported MOs, the quasi degenerate $22a_1$ HOMO and 32e SHOMO (second HOMO) can be correlated, on the basis of their similar localization percentages, to three degenerate t_2 levels in the more symmetric T_d group (see above). Interestingly, the empty $23a_1$ LUMO (lowest unoccupied MO) and 33e MOs are once more reminiscent of three degenerate t_2 levels in the more symmetric T_d group.

The quasi degeneracy of the occupied $22a_1$ and 32e MOs as well as of the unoccupied $23a_1$, $24a_1$, and 33e levels (see Table I) allows us to expect that the $Zn_4O(acetate)_6$ lowest energy electronic absorption transition reported by Kunkely and Vogler[4] at 216 nm in ethanol will be a band envelope rather than a single band. Actually, all the $a_1 \rightarrow a_1$, $a_1 \rightarrow e$, and $e \rightarrow e$ excitations are allowed by electric dipole selection rules in the C_{3v} symmetry. Moreover, it is worthwhile to mention that each excited configuration originates a number of singlet and triplet states ($^1A_1$ and $^3A_1$ from $a_1 \rightarrow a_1$; ^1E and ^3E from $a_1 \rightarrow e$; $^1A_1$, $^3A_1$, $^1A_2$, $^3A_2$, ^1E and ^3E from $e \rightarrow e$). To investigate the nature of the absorption band, a series of TS calculations relative to transitions between the occupied $22a_1$ and 32e MOs and the empty $23a_1$, $24a_1$ and 33e levels has been carried out. In Table II the average[22] triplet ($^3\Delta E$) and average[22] singlet ($^1\Delta E$) transition energies are reported. They have been computed by running two distinct spin-polarized

Table II. SCM DV Average[22] Triplet ($^3\Delta E$) and Average[22] Singlet ($^1\Delta E$) TS

excitation	$^3\Delta E$, eV	$^1\Delta E$, eV
$22a_1 \rightarrow 23a_1$	5.32	5.42
$22a_1 \rightarrow 24a_1$	5.96	6.00
$22a_1 \rightarrow 33e$	5.28	5.36
$32e \rightarrow 23a_1$	5.22	5.32
$32e \rightarrow 24a_1$	5.47	5.53
$32e \rightarrow 33e$	5.27	5.31

TS calculations for each excitation (a more detailed discussion of excitation energies as calculated by the employed method is given elsewhere).[23] As an example consider the excitation $22a_1 \rightarrow 33e$. A calculation of the configuration $(22a_1)^{\alpha}(22a_1)^{1/2\beta}(33e)^{1/2\alpha}$ would give[23a]

$$E^{\alpha}_{33e} - E^{\beta}_{22a_1} = {}^3\Delta E$$

where E^{α}_{33e} is the energy of the 33e MO containing an electron of spin α, etc. A further calculation on the configuration $(22a_1)^{\alpha}(22a_1)^{1/2\beta}(33e)^{1/2\beta}$ would give[23a]

$$E^{\beta}_{33e} - E^{\beta}_{22a_1} = \tfrac{1}{2}({}^3\Delta E + {}^1\Delta E)$$

The agreement between theoretical and experimental data is remarkable. In fact, the title molecule displays a strong absorption maximum (in ethanol) at $\lambda = 216$ nm (5.74 eV)[4] and the weighted mean value of the computed excitations to the singlet state is 5.42 eV. Moreover, it deserves to be pointed out that the excitations $22a_1 \rightarrow 24a_1$ and $32e \rightarrow 24a_1$ are reminiscent of an allowed $t_2 \rightarrow a_1$ transition in the more symmetrical T_d group accounting for a $2p \rightarrow 3s$ excitation on the central O′ atom and a charge transfer from the O″ 2p orbitals toward the 3s and 4s AOs of O′ and Zn atoms, respectively. In contrast to that, all the remaining computed transitions involve $p \rightarrow p$ excitations strongly localized on the O″ atomic centers. On an experimental ground, the absorption transition under investigation is definitely intense ($\epsilon = 62\,200$ mol^{-1} dm^3 cm^{-1})[4] and for sure, it cannot be ascribed to the $n \rightarrow \pi^*$ excitation of the acetate groups.[24] For the same reason, excitation involving triplet states can be assumed to contribute to a negligible extent. As a whole, we can expect the singlet $22a_1 \rightarrow 24a_1$ and $32e \rightarrow 24a_1$ excitations rather than the $p \rightarrow p$ ones to play a leading role in determining the high intensity of the experimental band. Incidentally, if we consider the weighted mean energy value of the $22a_1 \rightarrow 24a_1$ and $32e \rightarrow 24a_1$ spin-allowed transitions (5.69 eV), the agreement with experimental data (5.74 eV)[4] is excellent. On this basis, the assignment of the lowest energy absorption band of $Zn_4O(acetate)_6$ proposed by Kunkely and Vogler[26] is substantially confirmed, even though our theoretical results point out that the nature of this band is more complex and a nonnegligible contribution from a $2p \rightarrow 3s$ excitation localized on the central O′ is present.[27]

The presence of a low-lying empty MO ($24a_1$), highly localized on the O′ 3s AO, is particularly important because our basic assumption was that $Zn_4O(acetate)_6$ is a well-tailored molecular model of the crystalline ZnO. Now, in relation to the luminescence of other oxides containing closed-shell metal ions (but not with the d^{10} configuration), Jørgensen[28] proposed long ago that the

(22) The computed $^3\Delta E$ and $^1\Delta E$ values are weighted averages of transition energies to final states with the same spins but different symmetries.

(23) (a) Ziegler, T.; Rauk, A.; Baerends, E. J. *Chem. Phys.* **1976**, *16*, 209. (b) Ziegler, T.; Rauk, A.; Baerends, E. J. *Theor. Chim. Acta (Berlin)* **1977**, *43*, 261.

(24) The $n \rightarrow \pi^*$ excitations of the acetate groups are very weak and fall in the same spectral region ($\epsilon = 41$ mol^{-1} dm^3 cm^{-1} at 204 nm in EtOH)[25] as the lowest energy electronic absorption transition of $Zn_4O(acetate)_6$.

(25) Silverstein, R. M., Bassler, G. C., Morril, T. C., Eds. *Spectrometric Identification of Organic Compounds*, 3rd ed.; John Wiley and Sons: New York, 1974.

(26) The strong absorption band at 216 nm was assigned[4] to a ligand to metal charge transfer (LMCT) transition, lowered with respect to mononuclear Zn compounds by the interaction of the four Zn^{2+} 4s orbitals of the cluster.

(27) Despite the significant localization over the 4s Zn AOs, the largest contribution to the $24a_1$ MO comes, quite unexpectedly, from the O′ 3s AO (31%).

(28) Jørgensen, C. K. *Absorption spectra and chemical bonding in complexes*; Pergamon Press: Oxford, England, 1962.

Table III. Selected SCM DV Orbital Occupation Numbers in $Zn_4O(acetate)_6$

orbital	O′	O″	orbital	Zn
2s	1.64	1.69	3d	9.95
2p	4.22	4.43	4s	0.73
3s	−0.02	0.01	4p	0.91
3p	−0.25	−0.18	4d	0.28
Q	0.41	0.05		0.13
$\int_Q$	−1.19	−0.62		1.28

lowest energy absorption transition of these oxides corresponds to a 2p → 3s transition of the O^{2-} ion. The obtained result for the molecular compound forces us to question ourselves if a similar involvement of O 3s AOs is present at the bottom of the conduction band in ZnO (see the ZnO section).

As a whole, we agree with Blasse[5] that (i) the lowest energy electronic absorption transition of $Zn_4O(acetate)_6$ is of a rather complex nature, (ii) to explain the $Zn_4O(acetate)_6$ observed luminescence a leading role is played by the particular tetrahedral arrangement around the central oxygen atom, and (iii) the OZn_4O_{12} unit rather than the OZn_4 one is needed to satisfactorily describe the nature of the experimental band. Similar considerations should hold also for $Zn_4O(BO_2)_6$ where a similar structural arrangement around the central oxygen occurs.

At this point, we wish to comment briefly on the rather large (20 500 cm^{-1}, estimated in ref 6) Stokes shift shown by the title compound. Even though we do not intend to attempt any detailed discussion of the emission band, the qualitative explanation proposed by Kunkely and Vogler[4] needs to be slightly modified on the basis of our theoretical results. In fact, even though the $24a_1$ MO accounts for the totally symmetric linear combination of Zn 4s AOs,[29] resembling the empty a_1 "bonding" orbital assumed by Kunkely and Vogler[4] to be the excited orbital of the emission transition, the largest contribution to this level comes, as already stressed, from the O′ 3s AO.[27] As a final remark, the short decay time of the luminescence (τ = 10 ns)[4] clearly indicates that not only the absorption but also the emission process is spin-allowed.

A deeper insight into the electronic structure of $Zn_4O(acetate)_6$ can be gained by inspecting Table III, where the orbital occupation numbers, the gross atomic charges deriving from the Mulliken's analysis[18] of the occupied MOs and the electronic charge found in the nearest volume surrounding each atom ($\int_Q$) are reported. $\int_Q$ is particularly useful when, in order to achieve a detailed description of the metal–ligand covalent interactions, extended basis sets are employed. Actually, in the present case the inclusion of virtual levels provides additional degrees of variational freedom but at the same time it gives rise to nonphysical results (oxygen atoms positively charged) as a consequence of the negative population of diffuse 3s and 3p components of the oxygen basis set.[30-32] These problems can be overcome by using $\int_Q$. It is evident, from Table III, that the two types of oxygen (O′ and O″) are extremely different. In particular the O′ $\int_Q$ is definitely more negative than the O″ one, due to their different chemical environment. Moreover, it is worthy of note that despite the significant population of Zn 4p AOs (0.91 e) their contribution to the outermost MOs (see Table I) is poor.

The picture of the electronic structure of $Zn_4O(acetate)_6$ coming out from theoretical data nicely agrees with experimental findings. In particular, the XPS O_{1s} signal of the title molecule (see Figure 2) looks definitely asymmetrical with a less pronounced curvature at the lower BE side. The use of a deconvolution procedure, carried out by assuming the existence of two peaks and of a nonlinear Shirley-type background,[33] indicates the presence of a very weak O_{1s} peak at 531.0 eV BE and of an intense peak at 532.8 eV BE. The area ratio of the peaks (1/11) is very close to the expected theoretical ratio (1/12), leading us to ascribe the low-energy peak to O′. It is worthy of note that the BE of O′, lower than that of O″, is perfectly in agreement with the more negative $\int_Q$ of O′ than O″. Finally, we would like to emphasize that the measured BE of the O'_{1s} peak is very similar to that corresponding to the O_{1s} BE in ZnO (531.2),[34] confirming, on an experimental ground, that the $Zn_4O(acetate)_6$ is a very good molecular model of ZnO.

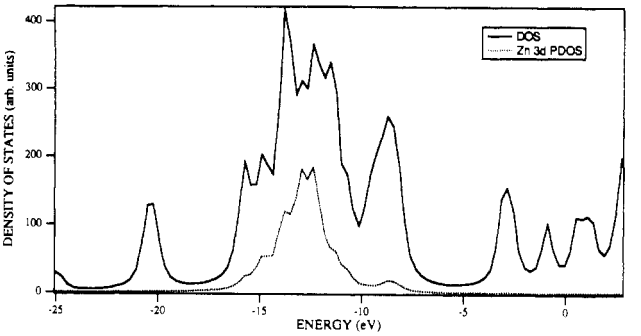

Figure 5. $Zn_4O(acetate)_6$ DOS + Zn 3d PDOS.

If we move to the analysis of the UV–PE data, the He I spectrum reported in Figure 4(bottom) can be conveniently divided in two distinct IE regions (from 9.5 to about 12 eV (region I) and the rest of the spectrum (region II)). The latter region consists of four band envelopes (C, D, E, and F in Figure 4) centered at about 12.4, 13.2, 13.9, and 15.2 eV. The ionizations expected in this region are those deriving from C–O, C–C, and C–H bonding levels.[35] The dramatic decrease in relative intensity of bands D and E and of the lower IE side of band F on passing from the He I to the He II ionizing source[36] (see Figure 4(top)) is in tune with such an assignment. In contrast to that, band C and the higher IE side of band F show an evident increase in relative intensity on switching from the He I to the He II ionizing source, the latter giving rise to the band F′ in Figure 4(top). The ionizations from Zn d AOs are known to lie between 17 and 19 eV in several Zn^{2+} compounds;[37,38] nevertheless, in $Zn(CH_3)_2$ the onset of the band due to the ionization from the corelike Zn 3d AOs have been observed at about 16.7 eV.[39] Now, in $Zn_4O(acetate)_6$ the valence atomic subshell photoionization cross sections significantly decrease on passing from the He I to the He II source[40] with the exception of the Zn 3d ones, which pass from 3.572 Mbarn to 7.292 Mbarn.[41] On this basis, the higher IE side of band F (F′ in Figure 4(top)) is due to the ionization from the Zn 3d AOs. Our theoretical results estimate their energy position to be between 12.5 and 15 eV (see Figure 5). Moreover, a TS calculation carried out for the inner $4a_2$ MO (almost completely localized on the Zn 3d AOs) gives a TSIE value of 15.33 eV, which is in good agreement with the proposed assignment.

The IE region I consists of two bands (A and B in Figure 4) centered at 9.91 and 10.55 eV and three evident shoulders (S, S′, and S″) on the higher IE side of band B. The full width at half-maximum of the band envelope A + B + S + S′ + S″ is about 1.7 eV. The energy region covered by the levels mainly localized on the O″ atoms (π_2, n^+, and n^-; see above), i.e., the MOs from

(29) The $24a_1$ MO accounts for a delocalized antibonding interaction between O′ and Zn atoms.
(30) Ellis, D. E.; Berkovitch-Yellin, Z. *J. Chem. Phys.* **1981**, *74*, 2427.
(31) Berkovitch-Yellin, Z.; Ellis, D. E. *J. Am. Chem. Soc.* **1981**, *103*, 6066.
(32) Casarin, M.; Vittadini, A.; Granozzi, G.; Fragalà, I.; Di Bella, S. *Chem. Phys. Lett.* **1987**, *141*, 193.
(33) Shirley, D. A. *Phys. Rev.* **1972**, *55*, 4709.
(34) Battistoni, C.; Dormann, J. L.; Fiorani, D.; Paparazzo, E.; Viticoli, S. *Solid State Commun.* **1981**, *39*, 581.
(35) Granozzi, G.; Casarin, M. In *Topics in Physical Organometallic Chemistry*; Gielen, M., Ed.; Freund: London, 1989; pp 107–162 and references cited therein.
(36) Rabalais, J. W., Ed.; *Principle of UV Photoelectron Spectroscopy*; Wiley Interscience: New York, 1977.
(37) Coksey, B. G.; Eland, J. H. D.; Danby, C. J. *J. Chem. Soc., Faraday Trans. 2*, **1973**, *69*, 1558.
(38) Orchard, A. F.; Richardson, N. V. *J. Electron Spectrosc. Relat. Phenom.* **1975**, *6*, 61.
(39) Bancroft, G. M.; Creber, D. K.; Ratner, M. A.; Moskowitz, J. W.; Topiol, S. *Chem. Phys. Lett.* **1975**, *50*, 233.
(40) The ionization of 2s O AOs cannot be obtained by using the He I source.[41]
(41) Yeh, J. J.; Lindau, I. Atomic Subshell Photoionization Cross Section and Asymmetry Parameters: $1 \le Z \le 103$. *At. Data Nucl. Data Tables* **1985**, *32*, 1.

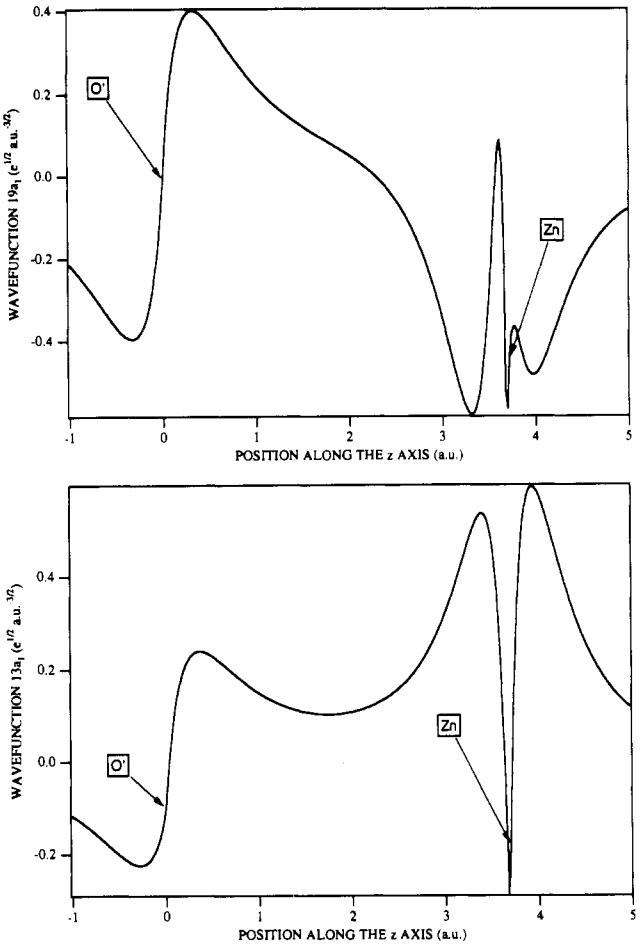

Figure 6. $19a_1$ MO (top) of $Zn_4O(acetate)_6$ along the z direction. $13a_1$ MO (bottom) of $Zn_4O(acetate)_6$ along the z direction.

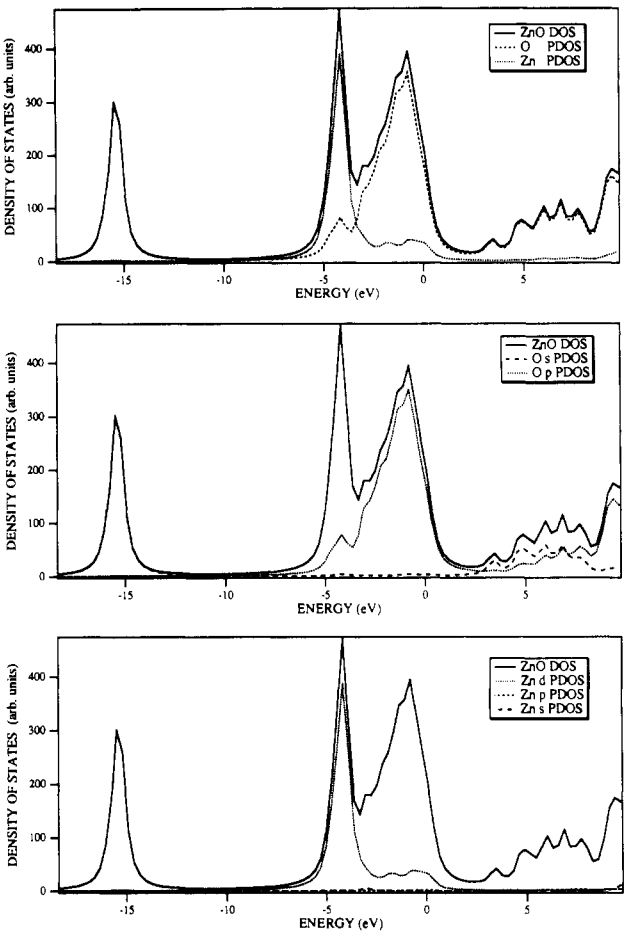

Figure 7. ZnO DOS (top), O PDOS (middle), and Zn PDOS (bottom).

$22a_1$ to $20a_1$ in Table I, is 1.6 eV. We propose to assign bands A and B, as a whole, to the ionization from the 12 highest lying MOs. In detail, believing in the TSIE order obtained from theoretical calculations, we assume that band A is due to the ionization from the $22a_1$ MO. At this point, we would like to emphasize that the numerical agreement between the IE of band A and the TSIE of the $22a_1$ MO is very good indeed. We do not propose any detailed assignment of band B because the remaining orbitals reported in Table I are (i) very close to each other and (ii) very similar in nature so that one cannot take advantage of the slight variations in relative intensity on passing from He I to the more energetic radiation.

The assignment of band C can be confidently made by taking advantage once more of theoretical data reported in Table I. In fact, the first 18 MOs ($22a_1$–$20a_1$) are separated by an energy gap 0.9 eV wide from two almost degenerate levels ($19a_1$ and 26e MOs). These orbitals are strongly localized on the O′ 2p (in the higher T_d symmetry they would transform as t_2) and the Zn 3d AOs. They are responsible for the Zn–O′ antibonding interaction (see Figure 6(top)). Incidentally, the bonding counterpart is accounted for by the $13a_1$ level (see Figure 6(bottom)), which, accordingly, is more localized on the Zn $3d_{z^2}$ AO. On the basis of the behavior of band C on passing from the He I to He II ionizing source as well as of the computed TSIEs relative to the $19a_1$ and 26e MOs (12.75, 12.82 eV, respectively), we confidently assign this band to the ionization from the MOs responsible for the antibonding interaction between Zn and O′ atoms.

ZnO. As we move to the analysis of theoretical results relative to ZnO, it is worthwhile to mention that very recently Mishra et al.[42] published a first principle investigation by means of the multiple scattered (MS) Xα cluster method of the electronic structure of the $(ZnO_4)^{6-}$ fragment in ideal T_d symmetry, as representative of crystalline ZnO. Their investigation follows a couple of papers which focused the attention on the same subject.[43] This gives us the opportunity to compare our results with other theoretical investigations obtained within the same approximation (the cluster one) even though it is useful to remember that in our calculations we used a larger cluster (OZn_4O_{12} vs ZnO_4), a more extended variational space, and a quite different theoretical scheme. Moreover, the Solomon group published in the recent past a detailed experimental investigation of the covalent bonding in $3d^{10}$ transition metal compounds,[44] allowing us to verify the quality of our theoretical data with respect to the literature ones.[42,43]

The first problem to be solved has been the choice of the correct number of electrons to be used to fill the DV self-consistent cluster energy levels. In principle, any number between 126 (the neutral cluster) and 144 (the ionic extreme) would be correct.[45] In the present contribution, taking into account both the rather ionic nature of ZnO and the need of handling a closed-shell system, we decided, as was done by Tossel[43] and Mishra et al.,[42] to use the ionic extreme.

Before going on to describe the obtained results, we want to emphasize that the cluster OZn_4O_{12} has a C_{3v} symmetry (see Figure 1b) rather than the T_d one of the smaller ZnO_4. The descent of symmetry will split t_2 and t_1 levels in $a_1 + e$ and $a_2 + e$, respectively. As a whole the 20 d orbitals of the four Zn atoms will originate the following linear combinations: $4a_1 + 2a_2 + 7e$.

(42) Mishra, K. C.; Johnson, K. H.; DeBoer, B. G.; Berkowitz, J. K.; Olsen, J.; Dale, E. A. *J. Lumin.* **1991**, *47*, 197.

(43) (a) Tossel, J. A. *Chem. Phys.* **1976**, *15*, 303. (b) Tossel, J. A. *Inorg. Chem.* **1977**, *16*, 2944.

(44) Didziulis, S. V.; Cohen, S. L.; Butcher, K. D.; Solomon, E. I. *Inorg. Chem.* **1988**, *27*, 2238.

(45) Müller, C. M.; Scherz, U. *Phys. Rev. B* **1980**, *21*, 5717.

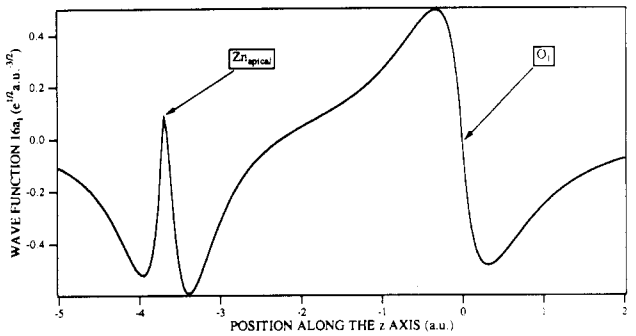

Figure 8. $16a_1$ HOMO along the z direction.

Among them the four d_{z^2} orbitals ("purely" t_2 in nature)[46] will transform as $2a_1 + e$, and two other levels of e symmetry will derive from the (d_{xz}, d_{yz}) and (d_{xy}, $d_{x^2-y^2}$) of the apical Zn atom. Finally, the remaining $2a_1 + 2a_2 + 4e$ orbitals will come from the linear combinations of d_{xz}, d_{yz}, d_{xy}, and $d_{x^2-y^2}$ localized on the three equivalent Zn atoms.

The computed total valence DOS and the Zn and O PDOS are reported in Figure 7, where the relative zero of energy is the eigenvalue of the $16a_1$ HOMO (−6.70 eV). The inspection of Figure 7(top) and -(middle) clearly indicates that the peak, quite distinct in energy, at about 15 eV is, according to previous theoretical data,[42,43,47,48] completely due to the atom-like O 2s AOs. Also the position of the peak due to the Zn 3d levels (~5 eV) is in tune with previous cluster calculations.[42,43] Unfortunately, a similar comparison with band structure calculations is not simple because several band structure investigations of the electronic properties of ZnO either do not explicitly include the 3d Zn levels[48,49] or determine, in a tight-binding band structure approach, the Zn 3d orbital parameters, by fitting them vs Xα calculations of the $(ZnO_4)^{6-}$ cluster.[50]

The agreement with experimental data[44] is not very good as far as the absolute energy position of the d band is concerned. On the other hand it is interesting to note that (i) the levels mainly t_2 in nature ($5a_1$ and $6a_1$ MOs) are the deepest orbitals among the 20 d levels and (ii) the energy range covered by the 20 d orbitals is 0.75 eV. In this respect our results are superior with respect to other cluster calculations[42,43] because not only the correct energy ordering of d levels is obtained (levels t_2 in nature more stable than the e ones) but also the energy dispersion of d AOs is in good agreement with experiment. This is a further confirmation that reliable results obtained by using the cluster procedure can be obtained only by using clusters sufficiently large and a variational space sufficiently expanded.[51]

A deeper insight into the covalent Zn–O interaction can be gained by making reference to the two bumps of the Zn d PDOS present in Figure 7(bottom). According to the qualitative bonding scheme proposed by Didziulis et al.[44] in their Scheme II (p 2244 of ref 44), they should represent the antibonding combinations between the oxygen 2p levels and the Zn 3d orbitals. In agreement to that, the $16a_1$ HOMO, mainly localized on the central O_1 and the apical Zn, accounts for the antibonding interaction between the p_z and d_{z^2} AOs of O and Zn atoms, respectively (see Figure 8).[52] Despite the fact that the cluster is not stoichiometric, the

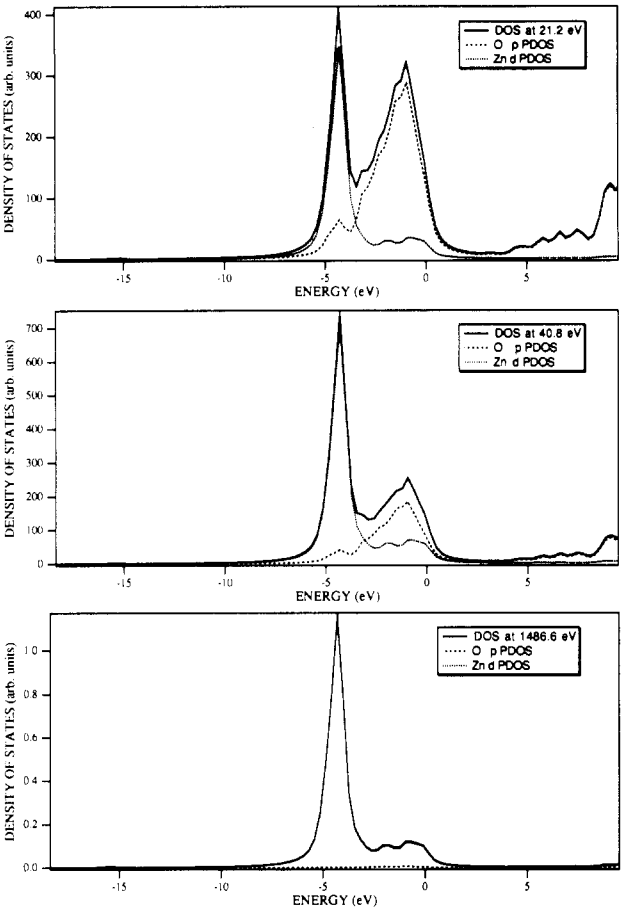

Figure 9. Theoretical Zn d PDOS + O p PDOS at 21.2 eV (top). Theoretical Zn d PDOS + O p PDOS at 40.8 eV (middle). Theoretical Zn d PDOS + O p PDOS at 1486.6 eV (bottom).

nonnegligible intensity of these bumps is a clear indication of the extensive mixing between Zn 3d and O 2p orbitals. Someone could argue that such an extensive mixing is the consequence of the "wrong" position of the d band, computed at too high an energy (too close to the O p band), but this is not the case. In order to demonstrate it, we normalized the Zn d PDOS and the O p PDOS with respect to the stoichiometry. Then, we multiplied them by the relative atomic subshell photoionization cross sections.[41] The obtained results are reported in Figure 9. The agreement with experimental data[44] is very good indeed. In particular, keeping in mind that the oxygen 2p photoionization cross section at 1486.6 eV is 0.24×10^{-3} Mbarn,[41] while the zinc 3d one at the same photon energy is 0.12×10^{-1} Mbarn[41] (2 orders of magnitude larger), the two bumps at low IEs in the spectrum recorded by Didziulis et al.[44] at 1486.6 eV are certainly due to the antibonding combinations between Zn 3d and O 2p AOs. Interestingly, the experimental XPS valence band of the molecular $Zn_4O(acetate)_6$ shows exactly the same features (see Figure 3), confirming the starting hypothesis that $Zn_4O(acetate)_6$ is a well-tailored molecular model of ZnO.

As already pointed out, one of our major concerns is the Zn–O covalency, and even if extensive, the interaction between the

(46) The d_{z^2} orbital for each Zn atom points toward an O atom (see Figure 1b).

(47) Chelikowsky, J. R. *Solid State Commun.* **1977**, *22*, 351.
(48) Kobayashi, A.; Sankey, O. F.; Volz, S. M.; Dow, J. D. *Phys. Rev. B* **1983**, *28*, 935.
(49) Ivanov, I.; Pollmann, J. *Phys. Rev. B* **1981**, *24*, 7275 and references cited therein.
(50) Lee, D. H.; Joannopoulos, J. D. *Phys. Rev. B* **1981**, *24*, 6899.
(51) Casarin, M.; Vittadini, A.; Ajò, D.; Granozzi, G.; Tondello, E. *Chem. Mater.* **1989**, *1*, 587.

(52) Despite the remarkable similarity between the $16a_1$ HOMO of the $OZn_4O_{12}^{18-}$ cluster in ZnO and the $19a_1$ MO of the $Zn_4O(acetate)_6$ (see Figure 6(top) and Figure 8) their relative energy position is highly different. On the other hand, as already pointed out, the first 18 MOs reported in Table I are strongly localized on the O″ p AOs, while the $19a_1$ MO is the highest energy MO localized on the O′ 2p AOs, that is on the oxygen atom representing the ZnO oxygen atoms. In other words, within the assumption that $Zn_4O(acetate)_6$ is well tailored to reproduce the main electronic features of the OZn_4O_{12} moiety in the crystalline ZnO, is the $19a_1$ level, rather than the $22a_1$ one, that would "correctly" represent the valence band edge of the solid. On the same ground, the empty $24a_1$ rather than the $23a_1$ LUMO could be associated to the conduction band bottom.

occupied Zn 3d and O 2p AOs cannot contribute to the overall covalent bond stabilization of ZnO. Elementary symmetry arguments and overlap considerations led Didziulis et al.[44] to assume that the interaction between the empty Zn 4s and 4p AOs and the occupied O 2p orbitals should play a leading role in the Zn–O bond formation. Such a qualitative analysis is confirmed by the present results which locate these levels on the higher IE side of the O 2p theoretical band, at about −2.5 eV in Figure 7.

After the analysis of data relative to occupied levels, it is noteworthy to focus our attention on the nature of the LUMO. First of all, within the cluster approximation, the LUMO $17a_1$ and the HOMO $16a_1$ are representative of the ZnO conduction and valence band edges, respectively. Their energy difference (−3.49 + 6.70 = 3.21 eV), or better the TS between them (−3.51 + 6.80 = 3.29 eV), can be assumed to be the fundamental band energy gap. The agreement with the experimental value (3.2 eV at room temperature) is surprisingly good. This result once again stresses the higher quality of our theoretical data with respect to the other literature cluster investigations[42,43] of the electronic structure of ZnO. Even more surprising than the good agreement between the HOMO–LUMO ΔE and the fundamental band energy gap was the localization of the $17a_1$ LUMO, which has a 85% contribution from the oxygen 3s AOs and a negligible percentage on Zn 4s AOs. To verify the relevance of the role played by the O 3s AOs, we carried out a further SCF calculation on the embedded cluster $OZn_4O_{12}^{18-}$ by using an O minimal basis set. The occupied MOs resulted only slightly shifted toward more negative energies (the $16a_1$ HOMO lying at −7.13 eV) with respect to those obtained by using the extended basis set. In contrast to that the relative energy position of the unoccupied orbitals is completely modified with the LUMO, almost completely localized on the Zn 4s AOs, lying at 0.22 eV.

To our knowledge the obtained data cannot be compared with any other literature calculation because this is the first time that an extended basis set is employed to investigate the electronic structure of ZnO. On the other hand, two different and completely independent facts lead us to be confident that the O 3s AOs are determining to obtain a satisfactory description of the electronic structure of ZnO: (i) the Jørgensen assignment[28] of the lowest energy absorption transition in metal oxides to a $2p \rightarrow 3s$ excitation localized on the O^{2-} ion (see above); (ii) the similarity between the computed electronic structure for ZnO and $Zn_4O(acetate)_6$, which in turn confirms itself to be a very good molecular model of ZnO.

Conclusions

The hypothesis that $Zn_4O(acetate)_6$ is a well-tailored molecular model of ZnO has been proved by using first principle local density molecular cluster calculations coupled to UV and X-ray photoelectron spectroscopies. In particular, it has been shown that the tetrahedral arrangement of four Zn atoms around the central oxygen present in $Zn_4O(acetate)_6$ provides a very good model of the oxygen chemical environment in ZnO. Moreover, theoretical results relative to the molecular compound allowed a detailed description of the nature of the lowest energy absorption transition, which in turn is mainly due to a charge transfer from the 2p O″ AOs toward the Zn 4s orbitals with a nonnegligible contribution from a $2p \rightarrow 3s$ excitation localized on O′. The significant involvement of the O′ 3s AO in the empty $24a_1$ level of $Zn_4O(acetate)_6$ is paralleled in ZnO by the very large localization percentage of the LUMO on the O 3s AOs (85%). As a whole the bonding scheme of ZnO is dominated by an extensive mixing between the 3d orbital of Zn^{2+} and the 2p level of the O^{2-} centers. Nevertheless, this mixing cannot determine, on its own, a covalent bond stabilization. The main source of bonding between Zn^{2+} and O^{2-} is due to the interaction of the empty 4s AOs of the former with the occupied 2p levels of the latter. The virtual 4p and 4d Zn orbitals do not seem to play any significant role in the overall Zn–O interaction as already found for $Zn_4O(acetate)_6$.

The good agreement between theoretical and experimental results relative to the electronic structure of ZnO is encouraging for future investigations of the electronic properties of substitutional transition metal impurities in ZnO.[53] In particular, preliminary results[54] relative to Cu^{2+} seem to indicate an electronic situation very close to that found for GaAs:Cu,[51] with the impurity 3d levels well deep in the valence band and a dangling bond hybrid[55] close to the valence band edge.

Acknowledgment. We are indebted to Prof. A. Vogler for kindly supplying a sample of $Zn_4O(acetate)_6$.

Registry No. $Zn_4O(acetate)_6$, 32334-63-7; ZnO, 1314-13-2.

(53) An experimental and theoretical investigation of the electronic properties of Co^{2+}, Ni^{2+} and Cu^{2+} substitutional impurities in ZnO is at the moment in progress in our laboratory.
(54) Casarin, M. Unpublished results.
(55) Zunger, A. In *Solid State Physics*; Ehrenreich, H., Turnbull, D., Eds.; Academic: New York, 1986; Vol. 39, p 275.